structure lends itself more readily to practical implementation than do the tandem structures proposed by Wang *et al.* [6]. Preliminary design data are presented for a YIG–As_2S_3–$LiNbO_3$ structure. Finally, we note that it might be more practical to provide a magnetic film rather than a magnetic substrate [3]. Studies of such a layered structure are underway, and we believe that this, too, could lead to a useful nonreciprocal isolator device.

ACKNOWLEDGMENT

The author wishes to thank W. K. Burns, T. G. Giallorenzi, and A. F. Milton for many stimulating discussions.

REFERENCES

[1] a) W. S. C. Chang and K. W. Loh, "Theoretical design of guided wave structure for electrooptical modulation at 10.6 μm," *IEEE J. Quantum Electron.*, vol. QE-8, pp. 463–470, June 1972.
b) D. Hall, A. Yariv, and E. Garmire, *Opt. Commun.*, vol. 1, p. 403, 1970.
c) D. Russo and J. Harris, *Appl. Opt.*, vol. 10, p. 2768, 1971.
[2] a) W. S. Chang, "Acoustooptical deflections in thin films," *IEEE J. Quantum Electron.*, vol. QE-7, pp. 167–170, Apr. 1971.
b) L. Kuhn, P. F. Heidrich, and E. G. Lean, *Appl. Phys. Lett.*, vol. 19, p. 428, 1971.
[3] P. K. Tien, R. J. Martin, R. Wolfe, R. C. LeCraw, and S. L. Blank, *Appl. Phys. Lett.*, vol. 21, pp. 394–396, Oct. 1972.
[4] L. D. Landau and E. M. Lifshitz, *Electrodynamics of Continuous Media.* Elmsford, N. Y.: Pergamon, 1960, pp. 331 *et seq.*
[5] J. Helszajn, *Principles of Microwave Ferrite Engineering.* New York: Wiley, 1969.
[6] S. Wang, M. Shah, and J. D. Crow, *J. Appl. Phys.*, vol. 43, no. 4, p. 1861, 1972.
[7] P. S. Pershan, *J. Appl. Phys.*, vol. 38, p. 1482, 1967.
[8] J. F. Nye, *Physical Properties of Crystals: Their Representation by Tensors and Matrices.* London, England: Oxford, 1957.
[9] R. A. Frazer, W. J. Duncan, and A. R. Collar, *Elementary Matrices.* Cambridge, England: Cambridge, 1952, p. 78.
[10] P. K. Tien, *Appl. Opt.*, vol. 10, p. 2395, Nov. 1971.
[11] M. V. Hobden and J. Warner, *Phys. Lett.*, vol. 22, pp. 243–244, 1966.
[12] L. Bornstein, *Physcial Tables*, vol. 2, part 8. Berlin, Germany: Springer, 1962, pp. 2–427.
[13] ——, *Tables* (New Series), group III, vol. 4a. Berlin, Germany: Springer, 1970, p. 344.

Periodic Structures and Their Application in Integrated Optics

WILLIAM S. C. CHANG, SENIOR MEMBER, IEEE

Invited Paper

***Abstract*—Periodic structures are used widely in integrated optics for input–output couplers, bandstop filters, modulators, directional couplers, and distributed feedback lasers. An analytical discussion and review of these devices is given based upon the coupled-mode transmission-line analysis. Experimental results and performance characteristics are presented to illustrate the special features of each type of device. Finally, the usefulness of transmission-line analysis to the understanding and the design of these devices is pointed out.**

I. INTRODUCTION

INTEGRATED optics is an ambitious attempt to apply thin-film and integrated electronics technology to optical circuits and devices [1]–[8]. One of its goals is to achieve sophisticated thin-film and fiber optical communication and data processing systems. We may envision that such systems will eventually be comparable to present microwave systems, complete with thin-film sources, detectors, waveguides, filters, directional couplers, modulators, etc. [7], [8]. Naturally, there is a great deal of similarity between microwave and integrated optical components. However, because of the shorter optical wavelength, many microwave techniques utilizing the matching of the transverse field variations for the fabrication of devices such as E–H tuners, magic T's, etc., are not applicable. Instead, techniques using periodic structures play a dominant role in integrated optical device fabrication. There are two major advantages in the use of periodic structures: a) although the individual interactions from each element in the periodic structure are small, their phase synchronized cumulative effects can be very large; and b) small amounts of random defects created in the fabrication process will not affect the characteristics of the device significantly. Applications of periodic structures in integrated optics have already led to the achievement of a number of devices such as the input–output grating coupler [9]–[12], the bandstop filter [13], distributed feedback lasers [14]–[16], modulators [17]–[22], and directional couplers [23].

Despite the fact that both the properties and the fabrication techniques of different devices using periodic structures vary a great deal, there is a considerable amount of similarity in their analyses. It is informative to review the properties of the various applications of periodic structures in integrated optics, one by one, from a unified coupled-mode transmission-line analysis point of view. Design data, experimentally measured properties, and performance characteristics will then be discussed to point out the special features of each

Manuscript received August 1, 1973. This work was supported in part by the NSF under Grant GK31854 to Washington University.

The author is with the Department of Electrical Engineering and the Laboratory for Applied Electronic Sciences, Washington University, St. Louis, Mo. 63130.

device. In order to present the comments in depth within a limited space, we shall limit our discussions here to one-dimensional periodic structures and shall exclude any discussion of optical nonlinear interactions.

II. A Perturbation Coupled-Mode Analysis

Consider the various structures shown in Fig. 1. All these structures have periodic variations of the dielectric constant in some regions of physical space. Within these regions, the periodic variation of the dielectric constant can be represented by

$$\Delta\epsilon(x, z) = \sum_{p=-\infty}^{\infty} D_p \exp\left(-j2\pi p \cos\phi x/L - j2\pi p \sin\phi z/L\right) \quad (1)$$

where p is designated here as the order of diffraction of the periodic structure. If either the amplitude of the periodic variation is small or the region within which the periodic structure exists (i.e., δ) is small, we can view the periodic structure shown on the right of Fig. 1 as a perturbation of the uniform thin-film waveguide shown on the left of Fig. 1.

The Maxwell's equations for the entire structure with $\partial/\partial y \equiv 0$ and with $e^{j\omega t}$ time variation can be reduced to the following well-known inhomogeneous wave equation [24], [25].

a) For TE Modes:

$$\left[\frac{\partial^2}{\partial x^2} + \frac{\partial^2}{\partial z^2} + k^2\epsilon(x)\right] E_y = k^2\Delta\epsilon(x, z)[u(x - t) - u(x - t - \delta)]\cdot[u(z) - u(z - l)]E_y \quad (2a)$$

where $H_y = E_x = E_z = 0$

$$H_x = -\frac{j}{\omega\mu_0}\frac{\partial E_y}{\partial z} \qquad H_z = \frac{j}{\omega\mu_0}\frac{\partial E_y}{\partial x}. \quad (2b)$$

b) For TM Modes:

$$\left[\frac{\partial^2}{\partial x^2} + \frac{\partial^2}{\partial z^2} + k^2\epsilon(x)\right] H_y = k^2\Delta\epsilon(x, z)[u(x - t) - u(x - t - \delta)]\cdot[u(z) - u(z - l)]H_y \quad (3a)$$

where $E_y = H_x = H_z = 0$

$$E_x = \frac{j}{\omega\epsilon_0\epsilon(x)}\frac{\partial H_y}{\partial z} \qquad E_z = \frac{-j}{\omega\epsilon_0\epsilon(x)}\frac{\partial H_y}{\partial x}. \quad (3b)$$

The term on the right-hand side of (2) and (3) is regarded here as the perturbation term; $k = 2\pi/\lambda$ is the free-space propagation wavenumber of plane waves; $\epsilon(x)$ is the relative dielectric constant shown in Fig. 1; u is the usual unit step function; and l is the total length of the periodic structure. In principle, the properties of any device using a periodic structure will be given by solutions of (2) and (3).

Solutions for the unperturbed structure (i.e., either $\delta = 0$ or $\Delta\epsilon = 0$) are well known [24]–[26]. They are the orthonormal set of TE and TM air modes, substrate modes, and guided wave modes. Using the notations given in [26] we shall designate any continuous mode (including both air and substrate mode) as

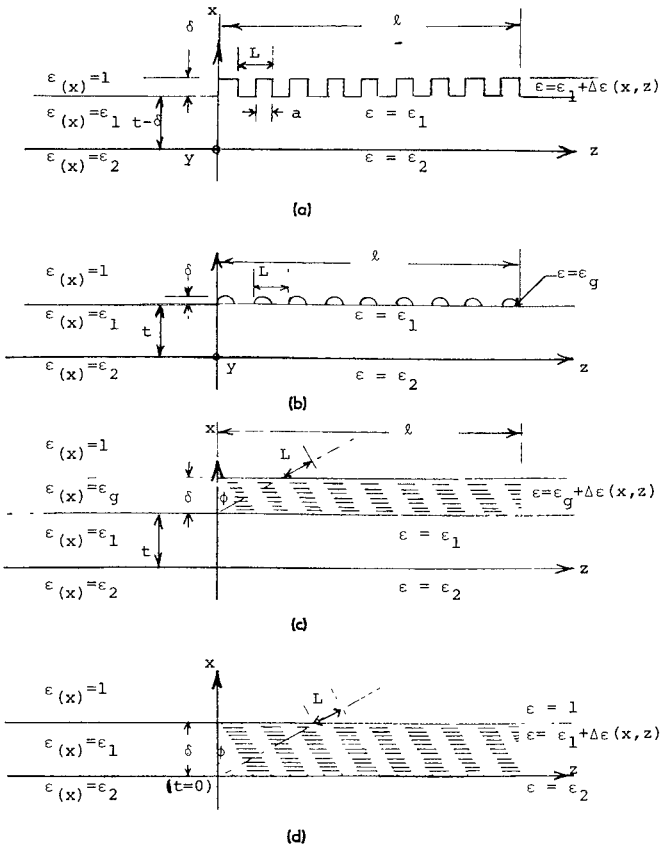

Fig. 1. Illustration of various periodic structures in integrated optics (ϕ is the angle of inclination of the grating fringes, $\phi = 90°$ for gratings with vertical fringes). (a) Etched grating. (b) Deposited grating. (c) Volume grating in the evanescent field region. (d) Volume grating in the guiding layer.

$$E_y = E(x, \beta)e^{-j\beta z}e^{j\omega t} \quad \text{for TE modes} \quad (4a)$$

$$H_y = H(x, \beta)e^{-j\beta z}e^{j\omega t} \quad \text{for TM modes.} \quad (4b)$$

The guided wave (i.e., discrete) modes shall be designated as

$$E_y = E_m(x)e^{-j\beta_m z}e^{j\omega t} \quad \text{for TE modes} \quad (5a)$$

$$H_y = H_n(x)e^{-j\beta_n z}e^{j\omega t} \quad \text{for TM modes.} \quad (5b)$$

Both the air and the substrate modes are modes of the radiation field.

If there is an incident wave in the form of one (or a combination) of these modes with a z variation $e^{-j\beta_0 z}$, each individual element of the periodic structure will scatter some of its energy into other modes. In other words, the scattered field, due to the perturbation of a single element, can be represented as a superposition of the continuous and discrete modes of the unperturbed structure. If we superimpose (i.e., sum) the contributions to a given mode from all the elements, we see that the total amplitude for any mode will, in general, tend to be very small because of the cancellations in phases of the individual contributions. For a few special modes when their phase variation, $e^{-j\beta z}$ (or $e^{-j\beta_m z}$), is equal to $e^{-j\beta_0 z}$ times $e^{-(j2\pi p \sin\phi\, z/L)}$, the individual contributions will add (i.e., be synchronized in phase). In these special cases, we recognize that significant transfer of power between the incident and the scattered mode can take place via the phase-synchronized pth-order diffraction of the periodic structure. Mathemati-

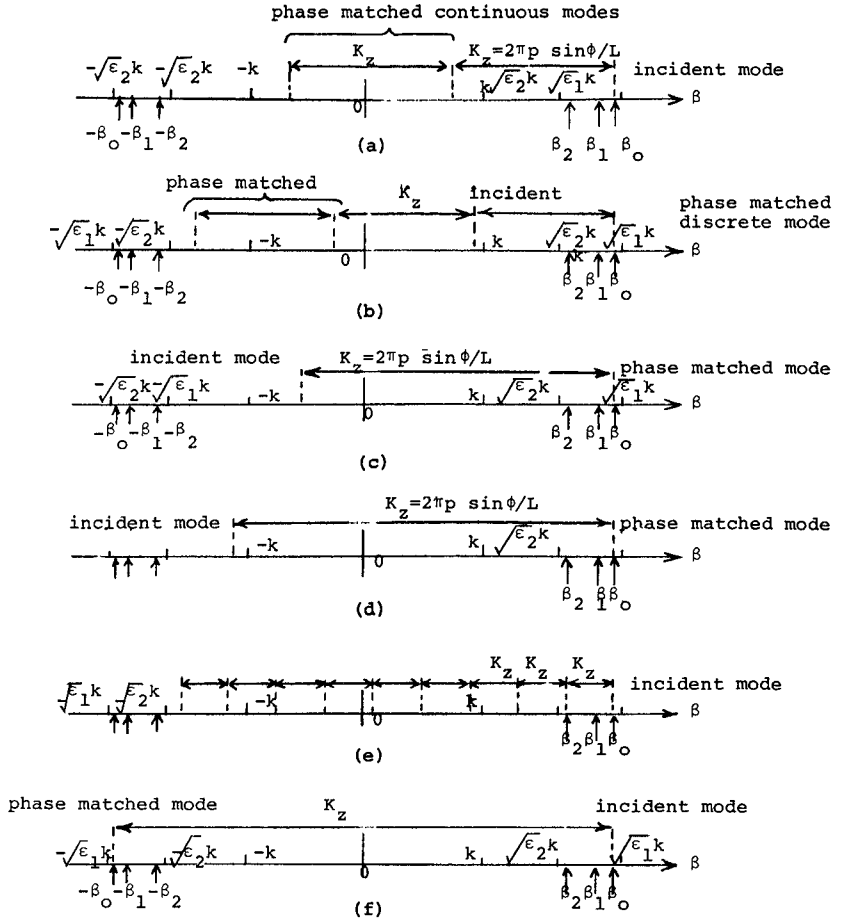

Fig. 2. Illustrations of collinear phase matchings. (a) Grating output coupler. (b) Grating input coupler (forward excitation by air modes). (c) Grating input coupler (backward excitation by air modes). (d) Grating input coupler (backward excitation by substrate modes). (e) Forward mode conversion. (f) Backward mode conversion.

cally, the condition for phase matching is usually written as

$$\beta = \beta_0 + 2\pi p \sin \phi/L \qquad \text{for continuous modes} \qquad (6a)$$

$$\beta_m = \beta_0 + 2\pi p \sin \phi/L \qquad \text{for discrete modes.} \qquad (6b)$$

Obviously, there may be more than one mode that satisfies the phase-matching condition. Fig. 2 illustrates different situations in which colinearly propagating modes may be phase matched for various kinds of grating periodicity.

In terms of (2) and (3), we see that the modes are solutions of the unperturbed homogeneous wave equations with $\Delta\epsilon \equiv 0$. When $\Delta\epsilon \neq 0$ and when there is an incident wave (consisting of one or more modes), all those modes that are not phase matched by (6) to the incident mode (or modes) can be neglected. The phase-matched modes are governed by the inhomogeneous (2) and (3), where the source term is simply $\Delta\epsilon$ times the incident mode. It is well known in microwaves that such an inhomogeneous equation can be considered simply as an inhomogeneous transmission line excited by a known source distribution. There are various microwave techniques for solving such an equation [27]–[29]. However, in optics it is worthwhile to emphasize that there is a difference between the transmission-line equivalent circuits for the discrete and the continuous (i.e., radiation) modes. For continuous modes, any scattered radiation field excited by the grating will be outgoing waves and will not reinteract with the grating once more to excite other modes. These solutions of the inhomogeneous equations always behave like a simple matched transmission line in the $\pm x$-directions excited by a known source confined within a small region of x. Any discrete mode is evanescent in the x-direction and will continuously be coupled to other modes through the periodic structure as it propagates along the z-direction. It is best described as a transmission line in the z-direction. When several modes are phase matched to each other, then they may be represented by transmission lines coupled to each other by the grating perturbation. These differences in transmission-line solutions are responsible for the different properties of the various devices described in the following sections.

III. The Grating Input–Output Coupler

A plane wave incident on an unperturbed thin-film waveguide will usually be accompanied by a reflected and a transmitted plane wave. A grating etched (or deposited) on the waveguide shown in Fig. 1(a)–(c) will diffract any discrete guided wave into outgoing radiation plane waves. This assortment of incident, reflected, and transmitted plane waves at a given angle of incidence θ (or any single diffracted outgoing plane wave at angle θ) is either a substrate mode or a linear combination of the degenerate even and odd air modes at the same β value with $\beta = \sqrt{\epsilon(x)}\, k \sin\theta$ or $\beta = \sqrt{\epsilon(x)}\, k \sin(\pi - \theta)$ [26]. Each mode (or a combination of degenerate modes) can be regarded as a transmission line.

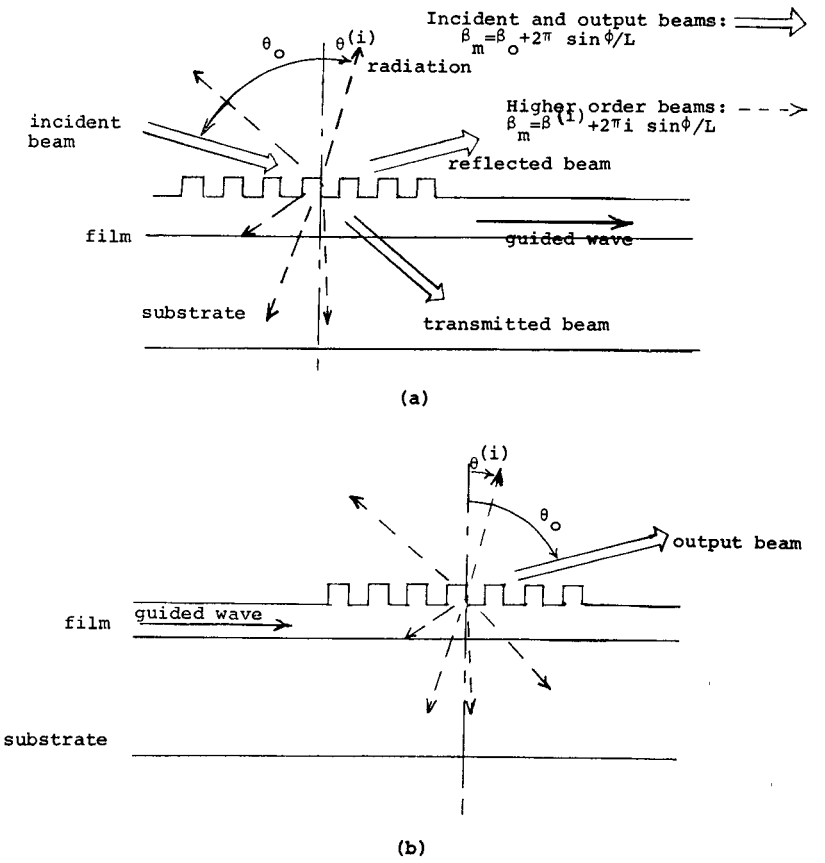

Fig. 3. Diffracted beams in a grating coupler. (a) Grating input coupler (excitation from the air). (b) Grating output coupler.

Consider now that there is a grating with an incident or diffracted plane wave at angle θ_0. β_0 and the grating periodicity, L, satisfy the phase-matching condition

$$\beta_m = \beta_0 + 2\pi \sin \phi/L \tag{7}$$

where $\beta_0 = k \sin \theta_0$ for plane waves in the air and $\beta_0 = n_2 k \sin(\pi - \theta_0)$ for plane waves in the substrate. The grating will convert part of the energy of the incident plane wave into the mth guided wave. Or, conversely, the grating will convert the energy of an incident mth guided wave mode into various diffracted plane waves at θ_0 and at $\theta^{(i)}$. In the former situation, the grating acts as an input coupler. In the latter case it is an output coupler. Naturally, there are other diffracted plane waves at angles very close to each $\theta^{(i)}$. They will be less intense than the plane wave at $\theta^{(i)}$ because the phase-matching condition is only partially satisfied. Therefore, in reality, each diffracted beam consists of a bundle of plane waves centered around each $\theta^{(i)}$. Similarly, the grating input coupler also will convert the energy of the incident plane wave into the mth guided wave, even if θ is slightly different from θ_0. The excitation efficiency will naturally be reduced when $\theta \neq \theta_0$. The angular range of either the diffracted beam or the incident excitation angle is called the beamwidth of either the diffraction or the excitation. Fig. 3 illustrates an input and an output grating coupler, the incident beam at θ_0, the output beam at θ_0, and the various higher orders of the diffracted beams at $\theta^{(i)}$.

It is informative to examine first the grating output coupler from the transmission-line point of view. Let V_m be the complex amplitude of the mth incident guided wave mode propagating in the $+z$-direction. The amplitude, V, of each of the phase-matched diffracted plane waves centered at $\theta^{(i)}$ (or at $\pi - \theta^{(i)}$) is proportional to V_m. Both the V's and the energy carried in each diffracted beam can be determined directly from the transmission-line analysis. Since the energy of the diffracted beams was extracted from the mth mode, V_m must decrease as the mode propagates along the grating. Thus we have [24]

$$\frac{\partial V_m}{\partial z} = -\left[\sum_i \alpha_{mi}\right] V_m = -\alpha_m V_m \tag{8a}$$

where

$$\alpha_m = \frac{k^4}{16\omega\mu_0}\left\{\sum_i \left[\frac{1}{\sigma_i} \mid C_a(i) \mid^2 + \frac{1}{\rho_i} \mid C_s(i) \mid^2 + \frac{1}{\rho_i} \mid C_s'(i) \mid^2\right]\right\}. \tag{8b}$$

Analytical expressions for C_a, C_s, and C_s' for TE_m modes in an etched coupler are given in (31) of [26]. Similar expressions can also be obtained for TM modes and for other structures. Each C_a term represents the diffraction loss in the form of a phase-matched outgoing radiation beam in the air with β values of the plane waves centered about $\beta^{(i)}$ where $\beta^{(i)} = \beta_m - (2\pi i \sin \phi/L)$ and $0 < \beta^{(i)} < k$. Each C_s term represents the diffraction loss in the form of an outgoing radiation beam in the substrate having the same value of $\beta^{(i)}$ as the corresponding C_a term. Finally, each C_s' term represents diffraction loss

with $k<\beta^{(i)}<n_2k$ (i.e., in the form of substrate modes without any companion radiation beam in the air).

From (8) it is clear that for a long enough grating ($l\gg 1/\alpha_m$) all the energy of the incident guided wave will eventually be diffracted out. Normally, only one of the outgoing beams at θ_0 is useful to us. Therefore, the maximum efficiency of an output grating coupler for the beam at θ_0 in the air is

$$\eta_{\text{out}} = \frac{1}{\sigma_0} |C_0|^2 \Big/ \sum_i \left[\frac{1}{\sigma_i}|C_a(i)|^2 + \frac{1}{\rho_i}|C_s(i)|^2 + \frac{1}{\rho_i}|C_s'(i)|^2\right]. \quad (9a)$$

Similarly, the maximum efficiency of an output coupler for the beam at θ_0 in the substrate is

$$\eta_{\text{out}} = \frac{1}{\rho_0} |C_0|^2 \Big/ \sum_i \left[\frac{1}{\sigma_i}|C_a(i)|^2 + \frac{1}{\rho_i}|C_s(i)|^2 + \frac{1}{\rho_i}|(C_s'(i)|^2\right]. \quad (9b)$$

Notice that $\eta_{\text{out}}\leqq 1$ in all cases.

For an input grating coupler, the mth mode receives energy from the incident plane wave as it loses energy to the diffracted beams. Thus (8) must be modified to account for the added energy:

$$\frac{\partial V_m}{\partial z} = -\alpha_m V_m + \nu A_p \quad (10)$$

where A_p is the amplitude of the electric field of the incident plane wave at the phase-matched angle and ν is the coupling coefficient from the incident beam to the guided wave obtained from the transmission-line analysis. Assuming that either the grating grooves or the incident beam begins at $z=0$ (i.e., $V_m=0$ at $z=0$), we obtain from (10)

$$V_m = \frac{\nu A_p}{\alpha_m}[1 - e^{-\alpha_m z}]. \quad (11)$$

The power carried by the normalized guided wave mode at a given z position is $V_mV_m^*$ while the power carried by the incident plane wave over a distance z is $[A_pA_p^*/2]z\cos\theta_0/\sqrt{\mu_0/\epsilon_0}n$ where n is the refractive index of the medium containing the incident beam. Thus the efficiency of an input coupler is

$$\eta_{\text{in}} = \eta_0 \frac{2(1 - e^{-\alpha_m z})}{\alpha_m z} \quad (12a)$$

with

$$\eta_0 = \nu\nu^*/(\alpha_m \cos\theta_0\sqrt{n\epsilon_0/\mu_0}) = \eta_{\text{out}}. \quad (12b)$$

The maximum value of η_{in} is $0.81\eta_0$ when $z=1.25/\alpha_m$.

From the preceding discussion it is clear that the highest maximum output coupling efficiency is 1 and the highest maximum input coupling efficiency for a plane wave incident on a linear grating is 0.81. In order to achieve this value we must: a) use a long grating length, l, for the output coupler ($l\gg 1/\alpha_m$) and an appropriate length for the input coupler ($l=1.25/\alpha_m$), and b) effectively reduce the coupling into all other unwanted beams (i.e., making $|C_0|\gg|C_a(i)|$ and $|C_s(i)|$ and $|C_s'(i)|$ for $i\neq 0$). The absolute magnitude of the coupling (e.g., the grating depth) controls only the length of the coupler needed for efficient operation; it does not affect the maximum efficiency.

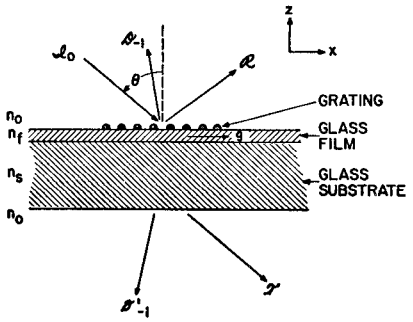

Fig. 4. A grating input coupler on a glass waveguide (taken from [9]). The incident beam (I_0), transmitted beam (τ), reflected beam (R), first-order diffracted beam in the air side (D_1), first-order diffracted beam in the substrate side (D_1'), and guided optical beam are shown.

If we define the beamwidth as the angular range, $\Delta\theta$, around θ_0 or $\theta^{(i)}$ within which the V of the diffracted plane waves will be larger than $1/\sqrt{2}$ of the V value at θ_0 or $\theta^{(i)}$, then from the solutions of V [26] we obtain

$$\frac{\sin(\cos\theta^{(i)}kl\Delta\theta/2\sin\phi)}{(\cos\theta^{(i)}kl\Delta\theta/2\sin\phi)} = \frac{1}{\sqrt{2}} \quad (13a)$$

for diffracted beam (or excitation) from the air, and

$$\frac{\sin(\cos\theta^{(i)}n_2kl\Delta\theta/2\sin\phi)}{(\cos\theta^{(i)}n_2kl\Delta\theta/2\sin\phi)} = \frac{1}{\sqrt{2}} \quad (13b)$$

for diffracted beam (or excitation) from the substrate. Note that long and shallow grating couplers yield narrow beamwidth.

Experimentally, Dakss *et al.* have demonstrated a deposited grating coupler shown in Fig. 4 for a glass waveguide at an efficiency of 40 percent [9]. Kogelnik and Sosnowsky have used a dichromatic gelatin holographic grating coupler and achieved an efficiency of 70 percent [10]. Dalgoutte obtained 70-percent efficiency using a backwardly excited deposited grating coupler [11]. Cheo used an etched grating on a GaAs waveguide and obtained 10-percent efficiency at the CO_2 laser wavelength [30]. Note the large variations in efficiency values (i.e., variations in η_0). These variations can be accounted for by the differences in the C coefficients in each case. Hence, analytical guidance [26], [31]–[33] is important in order to achieve efficient grating coupling in a given waveguide. It is also interesting to point out that, experimentally, a grating coupler can be evaluated most simply by using it as an output coupler, thereby determining its η_0.

There are several mechanisms available to us to make $\eta_0\cong 1$.

a) The modes of the laser (for input coupling only), the polarization of the incident wave, the grating groove shape, and the order of the grating [i.e., the D_p value in (1)] should be chosen so that $|C_0|$ is fairly large.

b) η_0 is one if the grating periodicity is chosen as shown in Fig. 2(d) and in [11] such that phase matching is achieved only for one substrate mode at the $|p|=1$ order (i.e., only one C_s' term exists).

c) If the refractive index of the film is high, then the C_s term is likely to be larger than the corresponding C_a term at

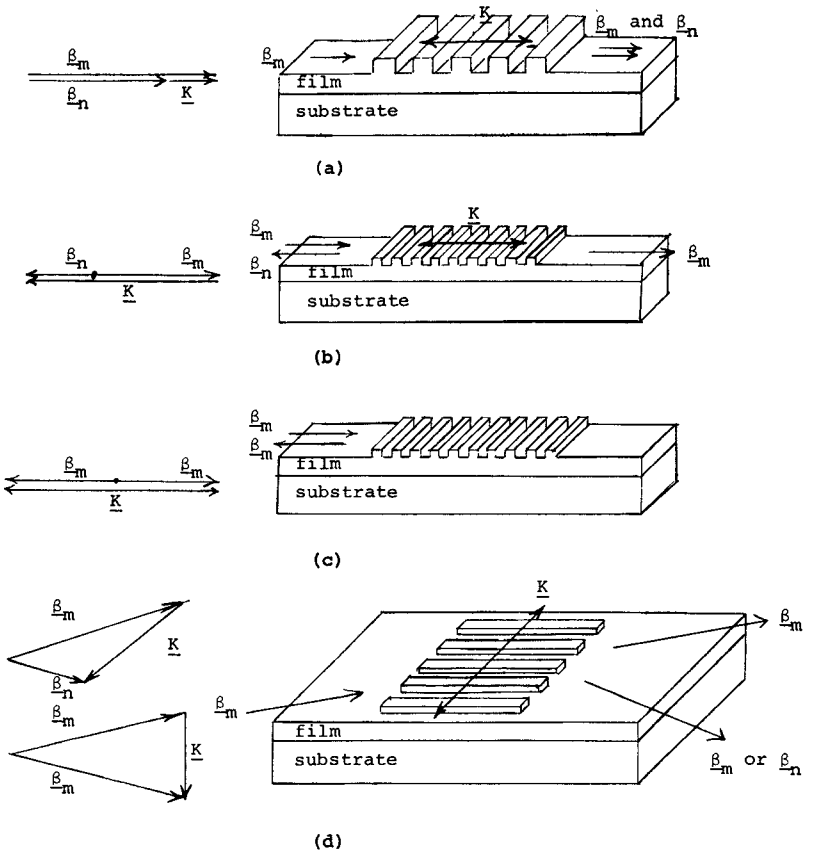

Fig. 5. Illustrations of grating mode converters and deflectors. (a) Forward mode converter. (b) Backward mode converter. (c) Reflector. (d) Bragg's deflector.

the same $\beta^{(i)}$. Hence, fairly large η_0 value can be obtained with β values in the zero to k range [see Fig. 2(c)] using the $|p|=1$ order and using air modes from the substrate side [26].

d) Other techniques may be used, such as using a holographic grating or using sinusoidal shaped grating grooves, to make the C coefficients very small at those unwanted orders of $|p|>1$. However, the holographic grating could also suppress the unwanted diffraction in either the substrate or the air side. The sinusoidal grating grooves will still have both the C_a and the C_s terms at the same value of β_0.[1]

IV. Periodic Mode Converters and Deflectors

Gratings can also be used to synchronously couple two propagating discrete modes. Consider the etched (or deposited) grating shown in Fig. 1(a). Let $\boldsymbol{K}$ be a vector perpendicular to the grating grooves with a magnitude $2\pi/L$. $\boldsymbol{\beta}_m$ and $\boldsymbol{\beta}_n$ are vectors representing the propagation wavenumbers along the directions of propagation of the mth and the nth mode. When the phase-matching condition $\pm\boldsymbol{K}=\boldsymbol{\beta}_m-\boldsymbol{\beta}_n$ is satisfied, the grating will convert the energy effectively from the mth mode to the nth mode and vice versa. Thus the grating is now a mode converter. If $\boldsymbol{\beta}_m$ and $\boldsymbol{\beta}_n$ are parallel to each other as shown in Fig. 5(a), it is a forward mode converter. If $\boldsymbol{\beta}_m$ and $\boldsymbol{\beta}_n$ are antiparalleled to each other as shown in Fig. 5(b), it is a backward mode converter. When $n=m$ in a backward mode converter as shown in Fig. 5(c), it is a reflector. When $\boldsymbol{\beta}_m$ and $\boldsymbol{\beta}_n$ are along different directions as shown in Fig. 5(d), it is a Bragg's deflector. Mode converters can also be used as directional couplers because the direction of propagation of two modes can easily be made to be different in thin films.

From the transmission-line point of view, the two transmission lines representing the nth and the mth mode are now coupled to each other via the first-order diffraction of the grating. Simultaneously, each of these two modes are also coupled to the continuous modes via higher order diffractions. We can estimate the diffraction losses to their radiation modes from (8). Compared to the grating input–output couplers, the diffraction losses now are much smaller and may not necessarily be the major contributor to the attenuation for the waveguide modes.

Let us designate the total attenuation rate, due to both diffraction and ordinary waveguide attenuation, as α_m and α_n. Then from the transmission-line formalism [23] the relation between the amplitudes of the mth and nth mode, V_m and V_n, is given by

$$\frac{\partial V_m}{\partial z} = -\alpha_m V_m + jK_{mn}V_n \tag{14a}$$

$$\frac{\partial V_n}{\partial z} = \mp\alpha_n V_n \pm jK_{nm}V_m. \tag{14b}$$

Here the mth mode is assumed to be propagating in the $+z$-direction. The nth mode is propagating at a small angle ψ with respect to the z axis. The upper sign in (14b) applies to forward deflection (or forward mode conversion) and the

[1] Recently, Tamir has shown that for grating groove depth $\cong\lambda_g/4$, $\eta_0\cong 1$, where λ_g is the equivalent wavelength in the grating region and the excitation is a plane wave from the air region. These deep gratings cannot be analyzed by the perturbation methods.

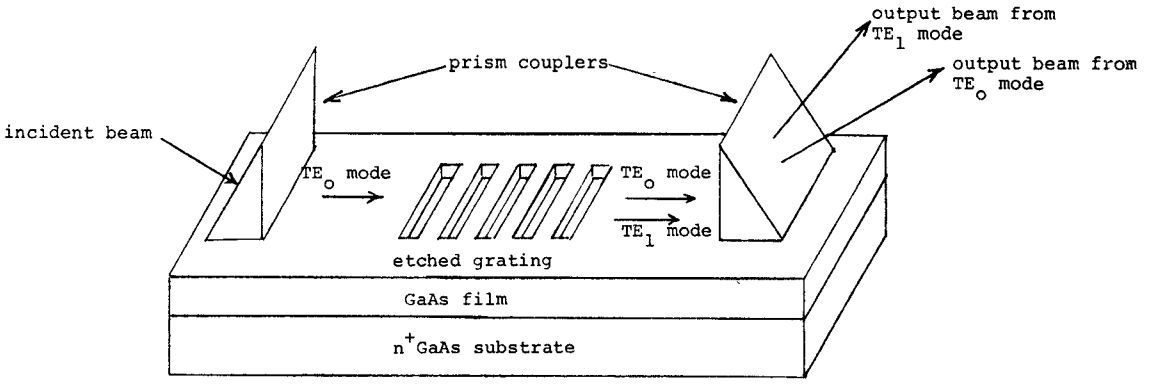

Fig. 6. Illustration of forward mode converter.

lower sign applies to backward deflection (or backward mode conversion). For structures with $D_1 = D_{-1}$ and for conversions and deflections with small angles of deflections ψ, the coupling coefficient K_{nm} is

$$K_{nm} = K_{mn} = \frac{k^2 D_1 \cos \psi}{4\omega\mu} \int_{t-\delta}^{t} E_m(x) E_n(x)\, dx. \quad (15)$$

For illustration, let us first consider the case of backward deflection and mode conversion where $\alpha_m = \alpha_n = \alpha$; the grating length is l; and $V_n = 0$ at $z = l$ and $V_m = 1$ at $z = 0$. In this case, the solution of (14) is:

$$V_m = \frac{\gamma \cosh \gamma(l - z) + \alpha \sinh \gamma(l - z)}{\gamma \cosh \gamma l + \alpha \sinh \gamma l} \quad (16a)$$

$$V_n = \frac{-jK_{mn} \sinh \gamma(l - z)}{\gamma \cosh \gamma l + \alpha \sinh \gamma l}, \qquad 0 \le z \le l \quad (16b)$$

$$\eta = \text{efficiency of conversion} = \frac{|V_n(z = 0)|^2}{|V_m(z = 0)|^2} = \frac{K_{mn}^2}{(\gamma \coth \gamma l + \alpha)^2} \quad (16c)$$

where

$$\gamma = \sqrt{\alpha_m^2 + K_{mn}^2}.$$

In the case of forward deflection and mode conversion, with $\alpha_m = \alpha_n$ and $V_n = 0$ at $z = 0$, we obtain

$$V_m = e^{-\alpha_m l} \cos (K_{mn} l) \quad (17a)$$

$$V_n = -je^{-\alpha_m l} \sin (K_{mn} l) \quad (17b)$$

$$\eta = \text{efficiency of conversion} = \left| \frac{V_n(z = l)}{V_m(z = l)} \right|^2 = \tan^2 (K_{mn} l).$$

Equations (16) and (17) predict that a controlled amount of energy can be deflected or converted out of the incident mode by controlling the depth of grating grooves and the length of interaction. Fig. 6 shows an experimentally fabricated grating forward mode converter at $\lambda = 10.6$ μm in a GaAs epitaxial waveguide [23]. Fig. 7 shows its calculated conversion efficiency compared to the experimental results. Note that in order to achieve high efficiency one must minimize α_m and α_n. The radiation loss may contribute significantly to α_m and α_n if we are not careful in designing the grating. For example, Fig. 8 shows the rapid increase of radiation loss for two particular GaAs waveguides when the grating grooves are deepened. The radiation loss in grating mode converters can be minimized by using shallow grating grooves, by using groove profiles to minimize D_p values for $p > 1$, and by designing the waveguide so that radiation modes are coupled to the discrete modes only at fairly high orders of diffraction.

V. Modulators Using Periodic Structures

Etched gratings achieved periodic changes in refractive index through their surface profile. One could also achieve periodic changes in refractive index by the electrooptical effect using a modulation voltage applied to a periodic electrode pattern or by the acoustooptical effect using acoustic waves at appropriate frequencies [17]–[21]. Since the changes of refractive index can now be controlled by either the applied modulation voltage or the amplitude of the acoustic waves, this type of deflector or mode converter can serve as an amplitude modulator or a switch. Experimental demonstration of the electrooptical Bragg's modulation and deflection was reported by Gia Russo and Harris [18] and by Polky and Harris [17] at $\lambda = 0.6328$ μm. In one case they used the electrooptical material nitrobenzene as the waveguide material and obtained amplitude modulation of 3 percent at 120 KHz using a 1-cm-long electrode with 30 V applied across the waveguide. In the second case, they used an interdigital periodic pattern electrode on a nitrobenzene filled waveguide and obtained 50-percent amplitude modulation at 8 KHz with a 5-mm-long electrode when 200 V was applied across the interdigital electrodes. Fig. 9 shows the modulator made by Polky and Harris. Experimental demonstration of acoustic mode conversion and Bragg's deflection at $\lambda = 0.6328$ μm was reported by Kuhn *et al.* in glass waveguides at 191- and 320-MHz acoustic frequency at a modulation efficiency of 66 and 45 percent, respectively [19], [20]. Fig. 10 shows the acoustooptical deflector made by Kuhn *et al.* Gfeller and Pitt reported collinear acoustooptical deflection in a polystyrene waveguide on a glass substrate [21]. Experimental demonstration of acoustic deflection and mode conversion at $\lambda = 10.6$ μm in GaAs epitaxial waveguide was also reported by Cheo [34]. Switching and modulation of light using periodic magnetooptical effects in garnet waveguide were accomplished by Tien *et al.* [22].

From the transmission-line point of view, the coupled-

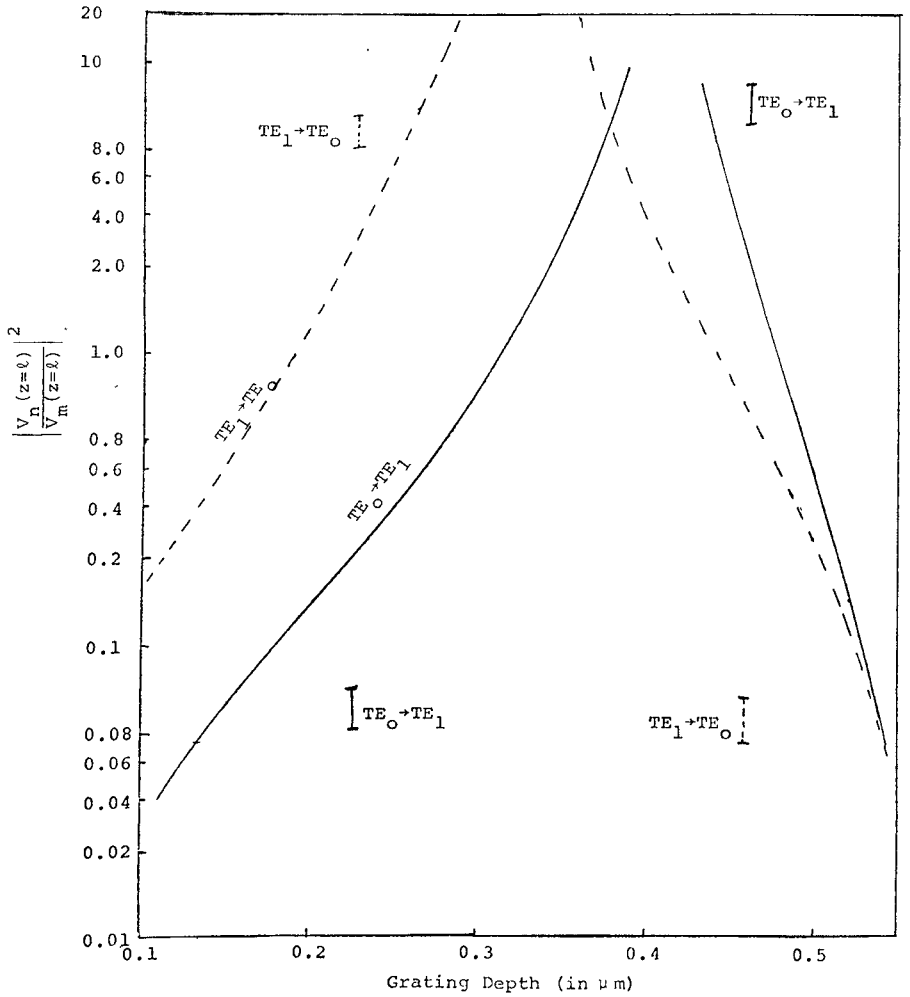

Fig. 7. Efficiency of a grating forward mode converter. GaAs/n^+ GaAs waveguide, $n_{film}=3.27$, $n_{sub}=2.14$ ($N=4\times10^{18}$), $t=29$ μ, $\alpha_1-\alpha_0=6$ dB/cm, $l=1$ cm, $L=731$ μm.

mode equation for the modulator is similar to those of the etched grating mode converter and deflector. Therefore, the solutions for modulation efficiency are the same as those given in (16) and (17) except that for electrooptical modulators

$$K_{mn} = \frac{k^2 n^4 r \mid V \mid}{2\pi\beta_m t} \left| \frac{\beta_m}{2\omega\mu} \int_0^t E_m E_n \, dx \right| \cos\psi \qquad (18)$$

where the modulation voltage V is applied across the waveguiding film of thickness t. n and r are the refractive index and the electrooptical coefficient of the waveguiding film, respectively. V is now a function of time.

In practice one would expect the K_{mn} coefficients for electrooptical modulators to be smaller than the K_{mn} coefficients for deep etched grating grooves because r is typically of the order of 10^{-12} m/V. An advantage of small K_{mn} is that the contribution to the attenuation coefficient, α_m, by radiation loss can usually be neglected. A disadvantage of small K_{mn} is that we need rather large values of K_{mn} to achieve efficient modulation constrained by: a) the required modulation drive power, and b) the available interaction length. This disadvantage is especially troublesome at long wavelengths such as 10.6 μm [35]. Thus from the point of view of the required RF power and voltage for a given depth and bandwidth of modulation, mode conversion will be an inefficient modulation (or switching) technique because of the small values achievable for $\int_0^t E_m E_n \, dx$. Bragg's deflection or reflection from the mth mode to a backward propagating mth mode is preferred. For a given modulator, (16), (17), and (18) allow us to optimize the modulator design so that we can get maximum deflection efficiency with minimum modulation drive power. For example, we may want to choose the thickness of the waveguide so that we can get the largest depth of amplitude modulation at a given applied voltage.

Similar conclusions can be drawn for acoustooptical modulators and switches. However, the acoustic waves will produce periodic Δn due to both variations of the density in the film and of the surface profile. The analysis will be more complicated. In general, electrooptical modulators will give the largest modulation bandwidth. Acoustooptical modulators can be operated with small RF power. However, their bandwidth is limited by the transit time of acoustic waves. Magnetooptical modulators are convenient to use but have moderate bandwidths.

VI. Periodic Bandpass Filters

When the frequency of the optical radiation is such that the phase-matching condition is satisfied for backward wave interactions, (16) predicts that all the energy in the mth mode

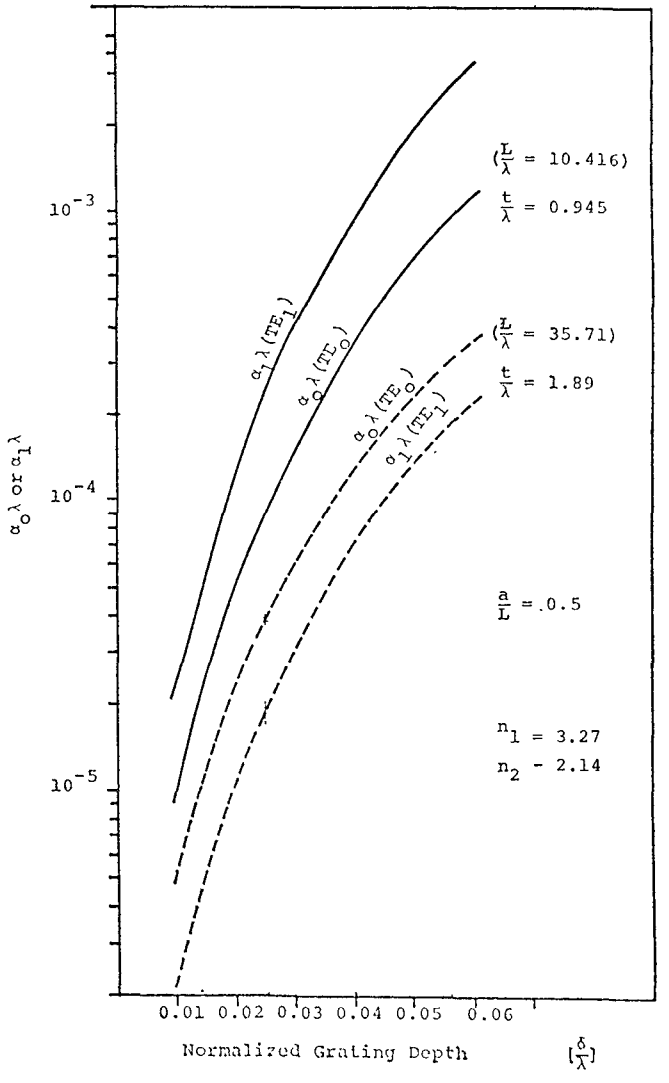

Fig. 8. α_0 and α_1 values of the TE_0 and TE_1 modes in a GaAs epitaxial waveguide with etched grating.

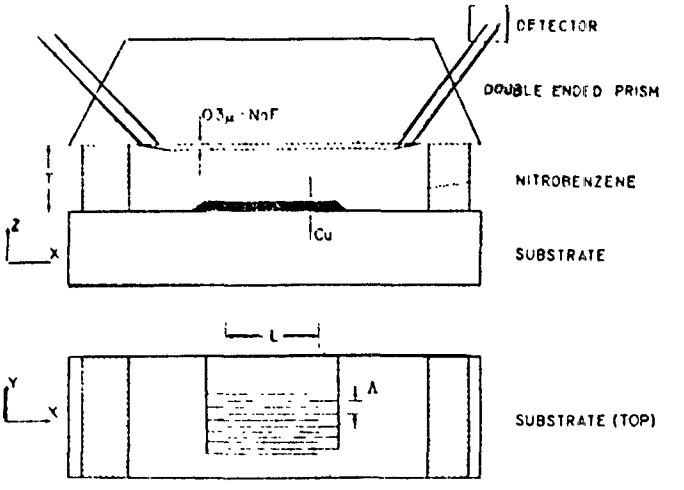

Fig. 9. Illustration of the thin-film modulator system used by Polky and Harris [17]. Guided modes propagate in the thin film of nitrobenzene while interdigital copper electrodes provide the modulating field. Shaded areas indicate sodium fluoride material.

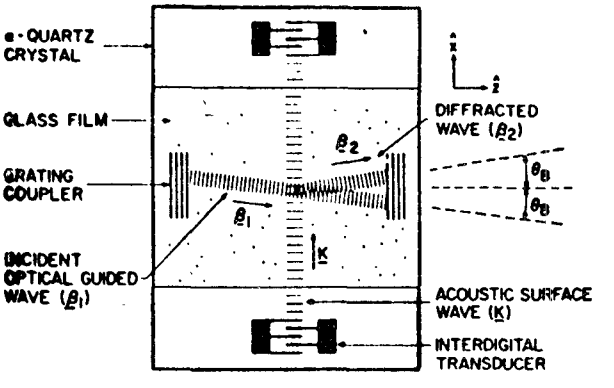

Fig. 10. Illustration of the acoustooptical deflector and modulator made in IBM [20].

will be reflected back for large l. In terms of the terminology used in traveling wave tubes, we say that this waveguide with an etched grating is now a periodic structure operated in its "stopband." When the frequency of the optical radiation does not satisfy the condition for backward interaction, the attenuation of the mth mode will be small. Therefore, periodic gratings can be used as bandpass filters. The analysis and the design of the bandpass filter are concerned with the width of the stopband, the insertion loss in the passband, and the magnitude of isolation in the stopband.

From the transmission-line point of view when two modes in opposite directions of propagation (most commonly a backward and a forward propagating TE_0 mode) do not satisfy the phase-matching condition exactly, they are coupled to each other through equations similar to (14) and (15):

$$\frac{\partial V_m}{\partial z} = -\alpha_m V_m + jK_{mn}V_n e^{j\Delta\beta z} \tag{19a}$$

$$\frac{\partial V_n}{\partial z} = \alpha_n V_n - jK_{mn}V_m e^{-j\Delta\beta z} \tag{19b}$$

and

$$\Delta\beta = \frac{2\pi}{L} - \beta_m - |\beta_n|. \tag{19c}$$

Here the mth mode is propagating in the $+z$-direction, and the nth mode is propagating in the $-z$-direction. α_m, α_n, and K_{mn} can be calculated according to (9), (15), and (18) and Section IV. The frequency is allowed to vary. The exact phase-matching condition corresponds to $\Delta\beta = 0$. In other words, $\Delta\beta$ is a measure of the deviation from the exact phase-matching condition. Without imposing the boundary conditions in z at this moment, we note that solutions of (19) must again be of the general form

$$V_m = (C_1 e^{-\gamma_0 z} + C_2 e^{+\gamma_0 z}) e^{j\Delta\beta z/2} \tag{20a}$$

$$V_n = (D_1 e^{-\gamma_0 z} + D_2 e^{+\gamma_0 z}) e^{-j\Delta\beta z/2} \tag{20b}$$

where for simplicity we have assumed $\alpha_m = \alpha_n = \alpha$. Substitution of (20) into (19) yields:

$$\gamma_0^2 = K_{mn}^2 + \left(\alpha + j\frac{\Delta\beta}{2}\right)^2. \tag{21}$$

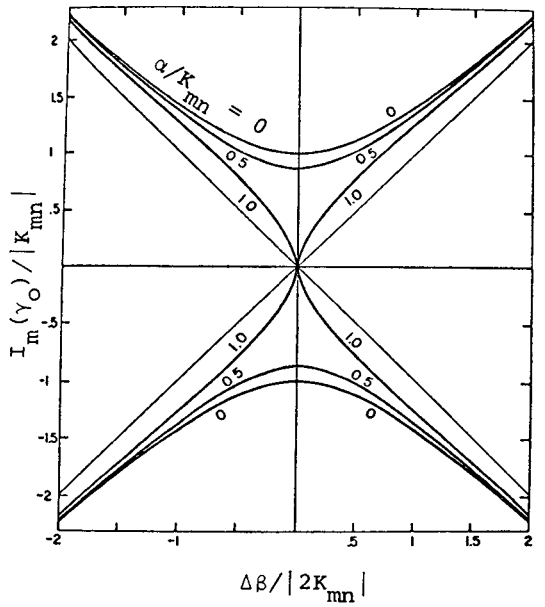

Fig. 11. Plot of $I_m(\gamma_0)$ versus $\Delta\beta$ in a periodically perturbed waveguide [36].

Equation (21) is the well-known dispersion relation of traveling wave structures. Kogelnik and Shank presented this result for the special case of $m=n$ in the coupled-wave analysis of distributed feedback lasers [36]. For an ideal waveguide with $\alpha=0$, (21) indicates that γ_0 is real (in other words the structure is in the stopband) whenever $|\Delta\beta| < 2|K_{mn}|$. Consequently, the stopband has a half-width of $2K_{mn}$. When $|\Delta\beta| > |2K_{mn}|$ $(\alpha=0)$, γ_0 is purely imaginary and the structure is in the passband. Fig. 11 shows the diagram of the imaginary part of $\gamma_0/|K_{mn}|$ versus $\Delta\beta/|2K_{mn}|$ when $\alpha=0$.

For a given structure we can use (21) to calculate the variations of the real part of γ_0 as $\Delta\beta$ is varied from the center to the edge of stopband, thereby evaluating the isolation obtainable within the stopband for a given length of the filter l. Similarly, in the passband, the real part of γ_0 determines the insertion loss of the filter for a given length l.

In the special case where $n=m$, the coupled-mode transmission-line analysis is, of course, just the perturbation analysis of the interaction of two space harmonics in the stopband. Elachi and Yeh presented extensive analysis of such a periodic structure from the space-harmonic point of view [37]. A detailed discussion of the properties of periodic structures in the stopband was given in their work. Dabby, Kestenbaum, and Paek presented a formalism that included more than two space harmonics [13]. The analysis presented here agrees with these results in the region where the grating can be treated as a perturbation. However, our method is also valid when the filtering is provided by two different modes (i.e., $m \neq n$).

Dabby, Saifi, and Kestenbaum have actually constructed such a filter [38]. The guides consisted of photoresist film with surface corrugation on fused silica substrate at a periodicity of 0.36 μm and at a depth of 500 Å. At $\lambda=1.064$ μm they obtained transition between complete cutoff and propagation by variation in the periodicity of the guide by ± 30 Å.

VII. Distributed Feedback Resonators and Lasers

Bandpass filters used the phase-matched interactions created by the periodic structure to reflect the incident mode. Such reflections naturally will occur in both directions. If the reflections that occur have the proper phase relationship so that they provide positive feedback, we will have then a distributed feedback resonator. If the waveguide has gain (e.g., a material impregnated with an appropriate dye) such that the gain exceeds the losses, we will have a distributed feedback laser.

A number of researchers have reported experimental demonstration of distributed feedback lasers. Shank, Bjorkholm, and Kogelnik obtained dye laser oscillation in which the feedback is achieved by pumping the dye with the fringes formed by the interference of two second-harmonic beams of a single-mode ruby laser [14]. Zory showed that laser oscillation can be obtained on the guided modes of leaky planar film waveguides by using a dye to provide the gain and backward diffraction from a spatially periodic modulation of the film thickness to provide the feedback [15]. Nakamura *et al.* reported laser oscillation in a GaAs thin-film waveguide pumped by a ruby laser; the grating was obtained by ion milling of photoresist patterns generated from the interference of two laser beams [16].

Kogelnik and Shank [36] gave an analysis of the distributed feedback laser, which is equivalent to the solution given in (20), subject to the boundary condition that $V_m(z=0) = V_n(z=l) = 0$; i.e.,

$$V_m = (\sinh \gamma_0 z) e^{j\Delta\beta z/2} \tag{22a}$$

$$V_n = [\sinh \gamma_0 (l - z)] e^{-j\Delta\beta z/2}. \tag{22b}$$

When there is enough gain and enough feedback to sustain oscillation, solutions given in (22) must also be the self-sustaining solutions of (19). Substitution of these two solutions into (19) yields the condition for the threshold of laser oscillation,

$$-\alpha - j\frac{\Delta\beta}{2} = \gamma_0 \coth \gamma_0 l. \tag{23}$$

Note that for a waveguide with gain, α is now a negative quantity. Each solution of (21) and (23) is an eigenvalue solution of (19). Substitution of these eigenvalues of γ_0 into (22) yields an eigenmode for the resonator. The α values needed to satisfy (21) and (23) simultaneously are the threshold gain. For a given length l and a given coupling coefficient K_{mn} each eigenmode has its characteristic field pattern, its threshold gain, and its characteristic resonance frequency. For example, Fig. 12 illustrates the oscillation frequencies and the threshold gain for a typical distributed feedback laser.

Much of the detailed properties of the solution of (23) are given in [36] and [37], and they will not be repeated here. We simply wish to point out here that, whenever there is only one discrete mode involved, the difference between the results given in [36] and the results obtained here is that we have given a method to evaluate K_{mn} for both etched periodic structures or periodic structures created by electrooptical or acoustooptical interactions. The coupling coefficient given by Kogelnik and Shank is accurate only for thick films. For thin-film waveguides their values of coupling coefficient will be too large because they assumed $\Delta\epsilon$ occurred in the entire environment including the waveguiding layers and all the evanescent field regions. Other researchers, using the space-harmonics method, have also obtained analyses of distributed feedback lasers including effects of surface corrugations, acoustooptical effects, etc. [37], [39]. Our method also allows us to evaluate

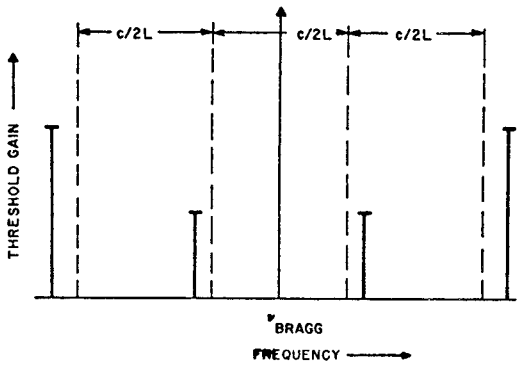

Fig. 12. Diagram illustrating the mode spectrum and required threshold gains for a distributed feedback [36].

the α caused by radiation loss. Moreover, for waveguides that can support more than one discrete mode, the oscillation mode pattern, the threshold condition, etc., will be given by solutions of (23), including all the possible combinations of discrete modes in backward diffraction. Recently, Bjorkholm, Sosnowski, Shank, and Kogelnik have reported distributed feedback lasers on anisotropic substrates [40], [41].

VIII. Summary

In retrospect, we see that the coupled-mode theory and transmission-line analysis developed originally for microwave circuits is very useful to integrated optics. The important parameters for the design and understanding of periodic structures in integrated optics are the attenuation rate α, the coupling factor ν, and the coupling coefficient K_{mn}. K_{mn} is determined by the overlap integral $\int E_m E_n \, dx$. By using the transmission-line analysis we could adjust the design of the structure both to optimize the coupling to a given radiation beam (or a given waveguide mode) and to minimize the other unwanted couplings. As a result, we could control the coupling efficiency, the conversion efficiency, the width of the stopband, etc. By the same kind of analysis, we could also assess laser resonant frequency, oscillation threshold, oscillation mode patterns in terms of the structure parameters such as waveguide thickness, refractive index, grating periodicity, grating depth, cavity length, etc. Obviously, limitations in space prevented us from giving a more detailed discussion of the characteristics and design procedures for each device. The readers are referred to the references listed at the end of this paper for detailed information.

Acknowledgment

The author wishes to thank Dr. F. J. Rosenbaum for his encouragement and stimulating discussions in the preparation of this manuscript.

References

[1] P. K. Tien, "Light waves in thin films and integrated optics," *Appl. Opt.*, vol. 10, pp. 2395–2413, 1971.
[2] E. T. Stepke, "Integrated optics," *Electro-Optical Systems Design*, vol. 5, pp. 18–23, 1973.
[3] S. E. Miller, "A survey of integrated optics," *IEEE J. Quantum Electron. (Part II) (Special Issue on 1971 IEEE/OSA Conference on Laser Engineering and Applications)*, vol QE-8, pp. 199–205, 1972.
[4] W. S. C. Chang, M. W. Muller, and F. J. Rosenbaum, "Integrated optics," in *Laser Applications*, vol. 2, M. Ross, Ed. New York: Academic, 1973.
[5] N. S. Kappany and J. J. Burke, *Optical Waveguides*. New York: Academic, 1973.
[6] R. A. Andrews, "Optical waveguides and integrated optics technology," Naval Res. Lab. Rep. 7291, Aug. 20, 1971.
[7] S. E. Miller, "Integrated optics: An introduction," *Bell Syst. Tech. J.*, vol. 48, pp. 2059–2070, 1969.
[8] S. L. Norman, "A look at optical integrated circuits," *Electro-Optical Systems Design*, vol. 3, pp. 22–28, Aug. 1971.
[9] M. L. Dakss, L. Kuhn, P. F. Heidrich, and B. A. Scott, "Grating couplers for efficient excitation of optical guided waves in thin films," *Appl. Phys. Lett.*, vol. 16, pp. 523–525, 1970.
[10] H. Kogelnik and T. P. Sosnowsky, "Holographic thin film couplers," *Bell Syst. Tech. J.*, vol. 49, pp. 1602–1608, 1970.
[11] D. G. Dalgoutte, "A high efficiency thin grating coupler for integrated optics," *Optics Commun.*, vol. 8, pp. 124–127, 1973.
[12] J. J. Turner *et al.*, "Gratings for integrated optics fabricated by electron-microscope," *Appl. Phys. Lett.*, vol. 23, pp. 333–334, Sept. 1973.
[13] F. W. Dabby, A. Kestenbaum, and V. C. Paek, "Periodic dielectric waveguides," *Optics Commun.*, vol. 6, pp. 125–130, 1972.
[14] C. V. Shank, J. E. Bjorkholm, and H. Kogelnik, "Tunable distributed-feedback dye lasers," *Appl. Phys. Lett.*, vol. 18, pp. 395–401, 1971.
[15] P. Zory, "Laser oscillations in leaky corrugated optical waveguides," *Appl. Phys. Lett.*, vol. 22, pp. 125–128, 1973.
[16] M. Nakamura *et al.*, "Laser oscillation in epitoxial GaAs waveguides with corrugation feedback," *Appl. Phys. Lett.*, vol. 23, pp. 224–225, 1973.
[17] J. N. Polky and J. H. Harris, "Electro-optic thin film modulator," *Appl. Phys. Lett.*, vol. 21, pp. 307–309, 1972.
[18] D. P. Gia Russo and J. H. Harris, "Electro-optic modulation in a thin film waveguide," *Appl. Opt.*, vol. 10, pp. 2786–2788, 1971.
[19] L. Kuhn, P. F. Heidrich, and E. G. Lean, "Optical guided wave mode conversion by an acoustic surface wave," *Appl. Phys. Lett.*, vol. 19, pp. 428–430, 1971.
[20] L. Kuhn, M. L. Dakss, P. F. Heidrich, and B. A. Scott, "Deflection of an optical guided wave by a surface acoustic wave," *Appl. Phys. Lett.*, vol. 17, pp. 265–267, 1970.
[21] F. R. Gfeller and C. W. Pitt, private communication from E. Ash, 1973.
[22] P. K. Tien *et al.*, "Switching and modulation of light in magneto-optic waveguides of garnet films," *Appl. Phys. Lett.*, vol. 8, pp. 394–396, 1972.
[23] K. Ogawa, W. S. C. Chang, B. Sopori, and F. J. Rosenbaum, "Grating mode converter/directional coupler for integrated optics," presented at the 1973 Spring Meeting of the Optical Society of America.
[24] D. Marcuse, "Mode conversion by surface imperfection of a dielectric slab waveguide," *Bell Syst. Tech. J.*, vol. 48, pp. 3187–3232, 1969.
[25] ——, *Light Transmission Optics*. New York: Van Nostrand, 1972.
[26] K. Ogawa, W. S. C. Chang, B. L. Sopori, and F. J. Rosenbaum, "A theoretical analysis of etched grating couplers for integrated optics," *IEEE J. Quantum Electron. (Part I)*, vol. QE-9, pp. 29–42, Jan. 1973.
[27] N. Marcuvitz, *Waveguide Handbook*. New York: McGraw-Hill, 1948.
[28] R. E. Collin, *Field Theory of Guided Waves*. New York: McGraw-Hill, 1960.
[29] W. H. Louisell, *Coupled Mode and Parametric Electronics*. New York: Wiley, 1960.
[30] P. K. Cheo, J. M. Berak, W. Oshinsky, and J. L. Swindal, "Optical waveguide structures for CO_2 lasers," *Appl. Opt.*, vol. 12, pp. 500–509, 1973.
[31] J. H. Harris, R. K. Winn, and D. G. Dalgoutte, "Theory and design of periodic couplers," *Appl. Opt.*, vol. 11, pp. 2234–2241, 1972.
[32] M. Neviere, R. Petit, and M. Cadilhac, "About the theory of optical grating coupler-waveguide systems," *Optics Commun.*, vol. 8, pp. 113–117, 1973.
[33] S. T. Peng, T. Tamir, and H. L. Bectoni, "Leaky-wave analysis of optical periodic couplers," to be published.
[34] P. K. Cheo and T. M. Reeder, "Acousto-optic interaction of a 10.6 μm guided-wave mode in GaAs thin film waveguide," presented at the 1973 Spring Meeting of the Optical Society of America.
[35] T. Ko and W. S. C. Chang, "A comparison of electro-optical modulation methods in GaAs epitaxial thin film waveguides at 10.6 μm wavelength," in *Proc. 1973 NSF Grantees Conf. Optical Communications*, May, 1973.
[36] H. Kogelnik and C. V. Shank, "Coupled wave theory of distributed feedback lasers," *J. Appl. Phys.*, vol. 43, pp. 2327–2335, 1972.
[37] C. Elachi and C. Yeh, "Periodic structures in integrated optics," *J. Appl. Phys.*, vol. 44, pp. 3146–3153, 1973.
[38] F. W. Dabby, M. A. Saifi, and A. Kestenbaum, "High frequency cutoff periodic dielectric waveguides," to be published.
[39] R. E. DeWames and W. F. Hall, "Conditions in distributed-feedback waveguides," *Appl. Phys. Lett.*, vol. 23, pp 28–29, 1973.
[40] J. E. Bjorkholm, T. P. Sosnowski, and C. V. Shank, "Distributed feedback lasers in optical waveguides deposited on anisotropic substrates," *Appl. Phys. Lett.*, vol. 22, pp. 132–134, 1973.
[41] H. Kogelnik, C. V. Shank, and J. E. Bjorkholm, "Hybrid scattering in periodic waveguides," *Appl. Phys. Lett.*, vol. 22, pp. 135–137, 1973.